Computers and Concrete, *Vol. 12, No. 1 (2013) 91-107*
DOI: http://dx.doi.org/10.12989/cac.2013.12.1.091

Reliability assessment of concrete bridges subject to corrosion-induced cracks during life cycle using artificial neural networks

Afshin Firouzi[1a] and Alireza Rahai[*2]

[1]*Construction Engineering and Management Group*, *Islamic Azad University*, *Science and Research Branch*, *Tehran*, *Iran*
[2]*Department of Civil Engineering*, *Amirkabir University of Technology*, *Tehran*, *Iran*

(Received February 26, 2012, Revised June 4, 2012, Accepted January 17, 2013)

Abstract. Corrosion of RC bridge decks eventually leads to delamination, severe cracking and spalling of the concrete cover. This is a prevalent deterioration mechanism and demands for the most costly repair interventions during the service life of bridges worldwide. On the other hand, decisions for repairs are usually made whenever the extent of a limit crack width, reported in routine visual inspections, exceeds an acceptable threshold level. In this paper, while random fields are applied to account for spatial variation of governing parameters of the corrosion process, an analytical model is used to simulate the corrosion induced crack width. However when dealing with random fields, the Monte Carlo simulation is apparently an inefficient and time consuming method, hence the utility of neural networks as a surrogate in simulation is investigated and found very promising. The proposed method can be regarded as an invaluable tool in decision making concerning maintenance of bridges.

Keywords: concrete; corrosion; random field; ANN; Monte carlo

1. Introduction

Deterioration of RC bridge decks due to frequently applied deicing salts is the main challenge of bridge owners worldwide. Existing Bridge Management Systems (BMSs) are based on condition rating data collected during routine visual inspections. In these systems, Markov chain models are incorporated in the core deterioration models of the system to predict the future bridge condition. Obviously there is a high degree of uncertainty in deterioration mechanisms and also inconsistency exists in inspectors' judgments. This was the motivation for the most researchers in the past decade to apply reliability methods for evaluation of deterioration of RC bridges. In the proposed reliability based maintenance management systems mechanistic deterioration models are utilized in a probabilistic framework to account for temporal variations of strength and loads (Frangopol *et al*. 1997). Nowadays in spite of considerable research concerning reliability analysis

∗Corresponding author, Professor, E-mail: rahai@aut.ac.ir
[a]Assistant Professor, E-mail: firouzi@aut.ac.ir

http://www.techno-press.org/?journal=cac&subpage=8 ISSN: 1598-8198(Print), 1598-818X (Online)

of bridges limited reported research exist in literature considering spatial variability of corrosion. In fact, in concrete structures, due to the spatial variability of workmanship, the material and dimensional properties of elements are not homogeneous. Furthermore, the environmental factors, e.g., surface chloride concentration, vary over the surface of the bridge components resulting in spatially variable corrosion damage symptoms. So prediction of the extent of damage, important from practical point of view in maintenance planning, needs more sophisticated reliability analysis, i.e., a random field instead of a random variable as the whole component parameter indicator, e.g., concrete compressive strength of the deck.

There are limited reported studies considering the effects of spatial variation of corrosion instructural reliability models (Li *et al*. 2004, Vu and Stewart 2005, Karimi *et al*. 2005, Sudret 2008). These research revealed the utility of considering spatial variability of corrosion parameters in prediction of the extent and likelihood of corrosion induced damage in RC structures. However, in most of these reliability analyses the propagation phase of the corrosion was not studied and primarily focused on the corrosion initiation phase or empirical models were incorporated for the propagation phase, e.g., prediction of crack width increase with time.

In the propagation phase, after initiation of surface cracks, their width will increase with time to a limit that spalling of concrete is prone. There are some models in the literature for corrosion-induced crack initiation phase (Liu and Weyers 1997, El Maaddawy and Soudki 2007), however the analytical model developed by Li *et al*. (2006) has the advantage of modeling crack width increase with time which is apparently more appropriate in defining serviceability limit states. This model is used in this study.

Furthermore, it can be noted that serviceability limit states, e.g., cracking, delamination, spalling, etc., in contrast to strength limit states, occur earlier in the service life of a bridge and demand more for repair and maintenance interventions. So the extent of cracked, spalled or delaminated area (length) seems an appropriate indicator of bridge condition and reliability.

In this paper, a two-dimensional temporal-spatial variable reliability analysis is conducted to predict the likelihood and extent of crack sofa hypothetical RC bridge deck exposed to deicing salts. In this regard spatial variability of corrosion model parameters is modeled using random fields, discretized with the midpoint method. These parameters include concrete material properties, concrete cover depth and surface chloride concentration. The number of discretized elements depends on how large the deck area is and which precision in discretization is desirable. However, the crude Monte Carlo simulation for prediction of crack width of a large number of discretized correlated elements during the whole life cycle is very time consuming and intractable. More difficulty arises especially in using the Li *et al*. (2006) analytical model for prediction of crack width which needs solving some nonlinear simultaneous equations in every iteration of Monte Carlo simulation for every discredited element in every time step. For tackling this problem the utility of neural networks are sought as surrogates for crude Monte Carlo in calculation of crack initiation time and crack width increase with time during service life of the bridge. Training of neural networks is based on hypercube sampling of concrete compressive strength and cover depth as the governing independent random fields. It was found that using well trained neural networks is very promising in attaining higher efficiency and precision of predicted crack width and extent of damage.

In the following sections of this paper, first analytical models pertaining to corrosion mechanism of reinforcement in concrete including initiation and propagation phases are presented. A brief introduction to random fields is the subject of the next section. After that, some notation regarding application and precision of feed forward neural networks is investigated. Furthermore

Latin Hypercube Sampling technique which is used for uniform selection of training samples of the neural networks is presented. And finally the proposed method is thoroughly explained, illustrated on a hypothetical bridge deck and the precision and efficiency of the results are discussed in conclusion section.

2. Corrosion mechanism

2.1 General

De-icing salts used in bridge decks cause ingress of chlorides through the concrete cover. The free chlorides in saturated concrete deactivate the natural protective oxide layer which is formed around the reinforcements by the strong alkalinity of pore solution. Once the protective layer has dissolved, if chloride concentration exceeds a threshold value and enough oxygen and moisture are present, corrosion is initiated. In the propagation phase, since the corrosion products have a volume of three to six times greater than the original steel, tensile stresses within the concrete increase which in turn result in cracking and spalling at the surface concrete.

2.2 Initiation phase

Numerous studies have found that the penetration of chlorides through concrete can be best represented by a diffusion process if the concrete is assumed to be relatively moist. In this case, the penetration of chlorides is given empirically by Fick's second law of diffusion if the diffusion is considered as one-dimensional in a semi-infinite solid; as expressed by Eq. (1)

$$\frac{\partial C}{\partial t} = D\frac{\partial^2 C}{\partial x^2} \tag{1}$$

In Eq. (1), C is the chloride concentration and D is the chloride diffusion coefficient of concrete. Crank's solution to Fick's second law of diffusion is represented as Eq. (2) (ACI 365 1R-00)

$$C(x,t) = C_0 + (C_{sa} - C_0)\left[1 - erf\left(\frac{x}{2\sqrt{D_a t}}\right)\right] \tag{2}$$

In general, the chloride concentration profiles obtained under different climates are used in mathematical models for obtaining parameters of Eq. (2). A plot of chloride concentration vs. penetration depth can often be closely described by Crank's solution to Fick's second law of diffusion. The curve-fitting results in these parameters: apparent diffusion coefficient, D_a, apparent surface chloride concentration, C_{sa} and the original chloride concentration, C_0 then $C(x,t)$ express the chloride content in depth of x at time t. These parameters are called apparent because obtained through curve fitting to the chloride concentration profiles of cored samples in which other penetration mechanisms have some effects. The corrosion of reinforcements is initiated when the chloride content, in steel bars embedment depth, X_c, exceeds a threshold value, $C_{cr,}$ which depassivates the steel embedded in the concrete provided that sufficient moisture and oxygen are present. In general, the uncertainty of governing parameters can be handled with random variables. There are lots of parameters, e.g. the wind direction, the sunlight effects, humidity of the micro-environment and etc., which affect the diffusion of the aggressive ions in the concrete, even in the

Table 1 Statistical description of variables

Variable	Scale of fluctuation $\theta_x = \theta_x$ (m)	Mean μ	C.O.V	Distribution	Reference
Concrete Cover(X_c), mm	3.5	50	0.2	Normal	Stewart & Mallard (2008)
Concrete Compressive Strength ($f_c^{'}$), MPa	3.5	35	0.2	Lognormal	Stewart & Mallard (2008)
Surface Chloride Concentration (C_{sa}), kg/m^3	3.5	3.5	0.6	Lognormal	Stewart & Mallard (2008)
Critical Chloride Concentration (C_{cr}), kg/m^3	-	0.9	0.19	Uniform (0.6-1.2)	Dupart (2007)
Reinforcement Size (D), mm	-	12	-	-	Li *et al.* (2006)
Porous Media around Reinforcement (d_0), μm	-	12.5	-	-	Li *et al.* (2006)
α_{rust}	-	0.57	-	-	Li *et al.* (2006)
Density of corrosion products (ρ_{rust}), kg/m^3	-	3600	-	-	Li *et al.* (2006)
ρ_{st} (kg/m^3)	-	7850	-	-	Li *et al.* (2006)
Poisson coefficient (v)	-	0.18	-	-	Li i (2006)

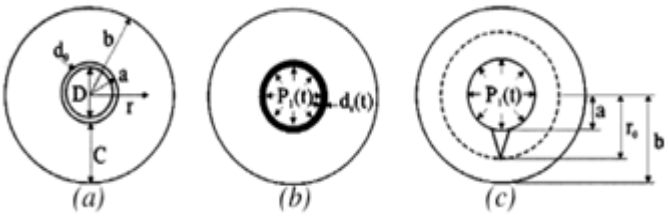

Fig. 1 Schematic representation of cracking process (Li *et al.* 2006)

opposite sides of a single concrete element. So without sufficient experimental data excreted from the existing structure under study, derivation of accurate statistical distributions for the aforementioned parameters, as random variables, will be cumbersome. However Dupart's (2007) concluding of various measurements in the literature for various environmental and workmanship classifications, made some general propositions. Based on such propositions (Dupart 2007, Stewart and Mullard 2008) the descriptive parameters of random fields and random variables are as shown in Table 1.

Considerable research has been undertaken on the corrosion-induced cracking process, with perhaps more numerical and experimental investigations than analytical studies (Chen and

Mahadevan 2008, Vu *et al*. 2005). For reliability calculations, a closed form mathematical model has a paramount advantage. In this regard, some models for the prediction of time to crack initiation of corroding reinforced concrete (RC) structures have been developed (Liu and Weyers 1997, El Maaddawy and Soudki 2007), but little has been developed on crack width growth with time. Some empirical models based on mathematical regression of experimental results exist in the literature. For example Vu *et al*. (2007) developed an empirical model for prediction of time of crack width increase up to 1 mm. This model is based on accelerated corrosion tests in the laboratory. However the applicability of such empirical models should be examined in other real situations.

In this paper, the analytical model developed by Li *et al*. (2006) is used for simulation of corrosion-induced crack width variation with time. The merit of this model is that it is directly related to the factors that affect the corrosion such as concrete geometry and property and corrosion rate.

In this model, as shown schematically in Fig. 1, concrete with embedded reinforcing steel bars is modeled as a thick-wall cylinder, where d_0 is the thickness of the annular layer of concrete pores (that is, a pore band) at the interface between the steel bars and concrete, D is the diameter of steel bar, and X_c is the concrete cover.

The inner and outer radii of the thick-wall cylinder are $a = (D + 2d_0)/2$ and $b = X_c + (D + 2d_0)/2$. When the steel bar corrodes in concrete, its products fill the pore band completely and a ring of corrosion products forms, the thickness of which, $d_s(t)$ (Fig. 1), can be determined from Eq. (3) as below (Liu *et al*. 1997)

$$d_s(t) = \frac{W_{rust}(t)}{\pi(D+2d_0)}\left(\frac{1}{\rho_{rust}} - \frac{\alpha_{rust}}{\rho_{st}}\right) \tag{3}$$

Where α_{rust} is a coefficient related to the type of corrosion products, ρ_{rust} is the density of corrosion products, ρ_{st} is the density of steel, and $W_{rust}(t)$ is the mass of corrosion products. $W_{rust}(t)$ increases with time and can be determined from Eq. (5) (Liu *et al*. 1997)

$$W_{rust}(t) = \left(2\int_0^t 0.105(1/\alpha_{rust})\,\pi D \times i_{corr}(t)dt\right)^{1/2} \tag{4}$$

Where $i_{corr}(t)$ is the corrosion current density (in μA/cm^2). In general, the formation of rust products on the steel surface will reduce the diffusion of the iron ions away from the steel surface resulting in reduced corrosion rates with time. For example Vu and Stewart (2005) suggested the following time dependent equation proposed for $i_{corr}(t)$

$$i_{corr}(t) = i_{corr}(1) \times 0.85(t - T_i)^{-0.3} \tag{5}$$

Where T_i is the time to corrosion initiation and $i_{corr}(1)$ is the corrosion current density in the first year after corrosion initiation which is based on concrete quality and can be calculated using Eq. (6) as below

$$i_{corr}(1) = \frac{27(1-w/c)^{-1.64}}{X_c} \tag{6}$$

Where w/c represents water to cement content ratio in the concrete.

According to Li *et al*. (2006) the growth of the ring of corrosion products exerts an outward pressure on the concrete at the interface between the rust products and concrete. Under this

expansive pressure, the concrete cylinder undergoes three phases in the cracking process: 1) not cracked; 2) partially cracked; and 3) completely cracked. In phase 1 (no cracking), the concrete can be considered as elastically isotropic so that the theory of elasticity can be used to determine the stress and strain distribution in the cylinder. For a partially cracked concrete cylinder, cracks are considered to be smeared and the concrete to be a quasi-brittle material, so that the stress and strain distribution in the cylinder can be determined based on fracture mechanics. When the crack penetrates to the concrete surface, the concrete cylinder completely fractures. Knowing the distribution of stress and strain, the crack width at the surface of the concrete cylinder can be determined as below

$$w_c = \frac{4\pi d_s}{(1-\nu_c)(a/b)^{\sqrt{\alpha}}+(1+\nu_c)(b/a)^{\sqrt{\alpha}}} - \frac{2\pi b f_t}{E_{ef}} \tag{7}$$

Where ν_c is Poisson's ratio of concrete and α (< 1) is the tangential stiffness reduction factor. According to Li *et al*. (2006) it is assumed that the residual tangential stiffness is constant along the cracked surface, that is, on the interval $[a, r_0]$, and represented by αE_{ef}, where E_{ef} is the effective elastic modulus of concrete which can be calculated as per Eq. (10) where φ_{cr} and E_c represent creep coefficient and elastic modulus of the concrete (Liu *et al*. 1997)

$$E_{ef} = \frac{E_c}{1+\varphi_{cr}} \tag{8}$$

In Eq. (7), the key variables are the thickness of corrosion products d_s, which is directly related to the corrosion rate (i_{corr}), and the stiffness reduction factor α, which is related to stress conditions and concrete property and geometry. Eq. (7) which is used in this paper has been verified by both numerical and experimental results (Li *et al*. 2006). In using this equation, one needs to calculate time dependent variables α and d_s. The former is determined solving simultaneous equations derived in Li *et al*. (2006) which are not repeated here for briefness purposes, while the later is calculated according to Eq. (3).

2.3 Effect of concrete quality

Various mechanical properties of concrete are usually correlated to compressive strength of concrete, a parameter which can be easily measured in practice. Referring to ACI 318-05, the concrete tensile strength (f_t) and modulus of electricity (E_c) is related to compressive strength as

$$f_t = 0.53\sqrt{f_c'} \text{ (MPa} \tag{9}$$

$$E_c = 4600\sqrt{f_c'} \text{ (MPa)} \tag{10}$$

The other important influencing parameter in studying corrosion in RC structures is the chloride diffusion coefficient. Several models have been developed to consider the influence of mix proportions on the chloride diffusion coefficient (Bamforth and Price 1996, Papadakis *et al*. 1996). The model developed by Papadakis *et al*. (1996) which appears to be the best fit to available literature is used in this study

$$D = D_{H_2O}\,0.15\,\frac{1+\rho_c\frac{w}{c}}{1+\rho_c\frac{w}{c}+\frac{\rho_c a}{\rho_a c}}\left(\frac{\rho_c\frac{w}{c}-0.85}{1+\rho_c\frac{w}{c}}\right)^3 \tag{11}$$

In this model *a/c* is the aggregate-to-cement ratio, ρ_c and ρ_a are the mass densities of cement and aggregates respectively and D_{H2O} is the chloride diffusion coefficient in an infinite solution (= 1.6×10^{-5} cm^2/s for NaCl). The water-cement ratio is estimated from Bolomey's formula for Ordinary Portland Cement (OPC) concretes as below

$$w/c = \frac{27}{f_c^{'}+13.5} \tag{12}$$

Where $f_c^{'}$ is the concrete compressive strength of a standard test cylinder in MPa.

3. Random fields

3.1 General

Effective parameters of the corrosion process exhibit a spatial variation in RC elements. For example, Poupard *et al*. (2006), studying an RC beam in marine exposure environment concluded that parameters like apparent diffusion coefficient and surface chloride concentration may have a high degree of spatial variation even in one element. Spatial variability of physical properties includes systematic spatial variation, e.g. variation of the mean value and standard deviation which is easily handled considering corresponding random variables, and random spatial variation. Random spatial variability of continuous media can be represented by the use of random fields (Chryssanthopoulos and Sterritt 2002). In the case of a large surface, a 2D random field can be used (Li *et al*. 2004, Stewart *et al*. 2006), while in the case of beam elements a 1D random field will be more appropriate (Engelund and Sorensen1998,Karimi *et al*. 2005, Sudert *et al*. 2007).

A simple model for a random field is a homogenous isotropic Gaussian field, where the random variables have a Gaussian distribution that does not change with direction or location, therefore the interdependency between two random variables defined at two points depends only on the distance between them.

The correlation function $\rho(\tau)$ determines the correlation coefficient between two elements separated by distance (τ) and is representative of the spatial correlation between the elements. As the distance between correlated elements becomes smaller, the correlation coefficient approaches unity as defined by the correlation function, and likewise, as the distance increases the correlation coefficient reduces. The Gaussian (or squared exponential) correlation function used herein is defined as (Stewart and Mullard 2008)

$$\rho(\tau) = exp\left[-\left(\frac{|\tau_x|^2}{{d_x}^2}\right) - \left(\frac{|\tau_y|^2}{{d_y}^2}\right)\right] \tag{13}$$

Where $d_x = \theta_x / \sqrt{\pi}$; and $d_y = \theta_y / \sqrt{\pi}$.

θ_x and θ_y are the scales of fluctuation for a two dimensional random field in x and y directions, respectively (VanMarcke 1984); and $\tau_x = x_i - x_j$ and $\tau_y = y_i - y_j$ are the distances between the centroid of element i and element j in the x and y directions, respectively.

The parameters of the Gaussian random field are the mean value μ, the standard deviation σ and the correlation length d_x and d_y.

Various methods of discretization of random fields have been proposed (Sudert and Der Kiureghian 2000). In the midpoint method, the random field needs to be discretised into *N*

elements of identical size and shape. The random field within each element is represented by a single random variable defined as the value of the random field at the centroid of the element and this value is assumed to be constant within the element. Following the discretisation, the covariance function can be replaced by an $n \times n$ covariance matrix C, for which the $(i, j)^{th}$ element is given by Eq. (13)

$$C_{i,j}=\rho_{i,j}\times\sigma^2 \tag{14}$$

If the distribution type is non-Gaussian, first a transformation into the Gaussian space is performed using the *Nataf* model (Nataf 1962). In this paper, regression formulas developed by Li and Der Kiureghian (1993) will be used for the mapping of the correlation coefficients to Gaussian space.

The matrix C is a symmetric completely positive matrix and the values on the diagonal refer to the autocorrelation and are equal to the variance of the Gaussian variable. The eigenvalue problem of the covariance matrix is C

$$C\psi_j = \mu_j\psi_j \tag{15}$$

A discretised random field, given by a vector p of length n, can be represented by the Karhunen-Loeve (KL) expansion in the form

$$H(x) = \overline{H(x)} + \sum_{j=1}^{r\le n}\psi_j\sqrt{\mu_j}\zeta_j \tag{16}$$

Where $\overline{H(x)}$ denotes the mean, ζ_j are uncorrelated standard normal (zero mean and unit variance) random variables. The mean $\overline{H(x)}$ and the eigensolutions μ_j and ψ_j are deterministic. The randomness of the field is only included in ζ_j. There are n eigensolutions, but in general it is sufficient to consider only the $r < n$ eigenfunctions with the largest eigenvalues, which give a good approximation of the random field.

4. Neural networks

An Artificial Neural Network (ANN) is an information processing paradigm that is inspired by the way biological nervous systems, such as the brain, process information. The key element of this paradigm is the novel structure of the information processing system. It is composed of a large number of highly interconnected processing elements (neurones) working in union to solve specific problems.

During the last decade approximations based on the concept of artificial neural networks are being introduced into reliability analysis. The primary motivation of using neural networks lies in their capability of good approximation of the results of time consuming repeated analyses of the Monte Carlo method. Papadrakakis *et al*. (1996) examined the utility of neural networks in reliability analysis of elastic-plastic structures and found this method very attractive. Hurtado and Alvarez (2001) compared performance of various types of neural networks in structural reliability analyses. Cheng *et al*. (2008) proposed ANN-based response surface approximation in highly nonlinear implicit performance functions utilizing the uniform design method for selection of a

training set of random variables. Hurtado (2002) demonstrated the applicability of Neural Networks for analyzing uncertainty in one dimensional stochastic finite element problems. Most and Bucher (2007) used a 2-D random field for representation of fluctuating material properties and then employed neural networks for approximating the response of a complicated model of coupled meshless and finite element analysis.

There exist a variety of alternatives to design a neural network. The focus of this study is set on feed forward neural networks which are already applied successfully in many fields of engineering. This was the first and arguably simplest type of artificial neural network devised. In this network, the information moves in only one direction, forward, from the input nodes, through the hidden nodes and to the output nodes. There are no cycles or loops in the network.

In the mathematical theory of neural networks, the universal approximation theorem states, that the standard multilayerfeed-forward network with a single hidden layer, which contains finite number of hidden neurons, is a universal approximator among continuous functions (Hornik 1991)

A commercially available software package, MATLAB Neural Network toolbox, is employed to facilitate the analysis. Hence, three layer ANNs are used here. In this work, two ANNs are employed to calculate: 1) crack initiation time; and 2) crack width increase with time during the service life of a hypothetical bridge deck. In this study the output layer of each ANN consists of a single neuron representing crack initiation age for the first ANN and time-dependent crack width for the other one. The input layer for the first ANN has two neurons representing the concrete compressive strength ($f_c^{'}$) and cover depth (X_c), as governing independent random variables of corrosion propagation. The input layer of the other ANN has one extra neuron, age as the other influencing input, to compute the crack width at that age.

A very important point for a sufficient network approximation is the design of the network architecture. Depending on the number of available training samples the number of neurons in the hidden layers has to be chosen in that way, whereas the so-called over-fitting is avoided. This phenomenon occurs, if the number of hidden nodes is too large for the number of training samples. Then the network can converge easier and fits well for the training data but it cannot generalize well for other data. Obviously if too few hidden units employed, high training error and high generalization error will occur due to underfitting. It is recommended to try many networks with different numbers of hidden units, estimate the generalization error for each one, and choose the network with the minimum estimated generalization error.

Finally based on trial and error 100 hidden neurons are used for both networks. Therefore the first ANN, computing the crack initiation time, is composed of 2 input, 100 hidden and 1 output neurons and the other ANN is composed of 3 input, 100 hidden and 1 output neurons.

Basically, learning is a process by which the free parameters (i.e., synaptic weights and bias levels) of a neural network are adapted through a continuing process of stimulation by the environment in which the network is embedded. In this study whilst in the hidden layer neurons use the sigmoid transfer function, a linear function is employed for the neurons of the output layers. The Levenberg-Marquardt algorithm is used to adjust the weights and biases of the network in order to minimize the mean squared error between the resultant values solving the equations of the analytical model and that predicted using the ANN models. The minimization of the mean squared error proceeds until it converges to within a preset tolerance for all test points.

The selection of training datasets is an important issue in the context of establishment of the ANN model. The main aim in the selection of training datasets is to make the selected training data as uniformly as possible to cover the entire design space. Therefore, Latin hypercube

sampling is adopted herein to select the training datasets for establishing an ANN model.

5. Latin hypercube sampling

Latin hypercube sampling was first proposed by McKay *et al*. (1979). However, various improvements have been developed for increasing the efficiency and precision of this method (Olsson *et al*. 2003). In this method, the desired accuracy of the estimated distribution function determines the number of realizations required. Let *N* denote the required number of realizations and *K* the number of random variables. The sampling space is then *K*- dimensional. An *N*×*K* matrix *P*, in which each of the *K* columns is a random permutation of 1, *N*, and an *N* × *K* matrix *R* of independent random numbers from the uniform (0, 1) distribution are established. These matrices form the basic sampling plan, represented by the matrix *S* as

$$S = \frac{1}{N}(P - R) \tag{17}$$

Each element of *S*, s_{ij}, is then mapped according to its target marginal distribution as

$$\hat{x}_{ij} = {F^{-1}}_{x_j}(s_{ij}) \tag{18}$$

where ${F^{-1}}_{x_j}$ represents the inverse of the target cumulative distribution function for variable *j*. Then samples are spread over the entire sampling space as the generation of the LHS plan requires one image from each row and each column. If *N* realizations from the entire sampling space had been chosen completely at random, as in crude Monte Carlo sampling, there is a risk that they would form a cluster and some parts of the sampling space would not be investigated.

6. Description of method

The main purpose of this paper is to present a method for prediction of extent and likelihood of corrosion-induced severe cracking using ANNs. In this regard first the adapted computational procedure is briefly introduced and then application of the method and the results are investigated

6.1 Computational procedure

Step 1-Use midpoint method for descretization of independent random fields; e.g. concrete cover (X_c), concrete compressive strength ($f_c^{'}$) and surface chloride concentration (C_s); into N_T correlated random variables and construct associated covariance matrix *C* for every random field.

Step 2-Use regression formulas developed by Li and Der Kiureghian (1993) for the mapping of the correlation coefficients to Gaussian space.

Step 3-Use the Karhunen-Loeve transformation in order to simulate vector random fields

Step 4-Simulate N_{sim} realization of uncorrelated standard normal random variables (ζ_j) using Latin hypercube sampling. This means simulation of N_{sim} realizations of random fields.

Step 5-Simulate N_{sim} realization of other random variables, e.g., critical chloride concentration.

Step 6-Calculate corrosion initiation time, T_{int} for every descretized element in every realization of simulation using Eq. (2).

Step 7-Calculate crack initiation time and crack width of every decartelized element during a prescribed lifetime of deck in every realization of simulation using Eq. (7) and solving simultaneous equations of Li *et al*. (2006).

Step 8-Train ANNs with the simulated values of previous step as target values.

Step 9-Trained ANNs can work as a surrogate to time-consuming Monte Carlo method for calculation of the extent and likelihood of severely cracked area of deck.

6.2 Hypothetical bridge deck specification

A spatial time-dependent reliability analysis is developed for a hypothetical RC bridge deck with 12 m length and 10 m width exposed to de-icing salts. The analysis considers corrosion initiation and then propagation of corrosion-induced cover cracking in the top surface of the deck until a crack width of 0.3 mm is reached, which is the prescribed limit crack width in Duracrete (2000) and ACI-318-05. A 2D homogenous Gaussian random field is applied to consider the spatial variability of concrete compressive strength. This means that related properties of concrete, e.g. chloride diffusion coefficient, concrete tensile strength and concrete effective modulus of elasticity, water-cement ratio and corrosion density rate are the dependent random fields as per equations presented in Sections 1.2 and 1.3 of this paper. Furthermore, concrete cover depth and surface chloride concentration are represented by independent random fields to account for spatial variations of these parameters.

According to Stewart and Mullard (2008) the scale of fluctuation of these random fields is approximately 3.5 m (d_x = d_y = 2.0 m). In Table 1 full statistical description of random fields, random variables and deterministic variables are illustrated**.** The 2D random field is discretized into square elements of size Δ = 0.5 m, resulting in $N_T = 480$ elements. For every realization of Monte Carlo simulation the proportion of deck area with crack widths exceeding limit crack width at the time of t is calculated as follows

$$X(t) = \frac{n_f[t>Tint\,(j)+Tsc\,(j)]}{N_T} \tag{19}$$

In Eq. (19) corrosion initiation time of element j is denoted by $\mathrm{Tint}\,(j)$, this element's crack width (w_c) reaches to 0.3 mm in $\mathrm{Tsc}(j)$ years after corrosion initiation and $\mathrm{n_f}$ is the total number of

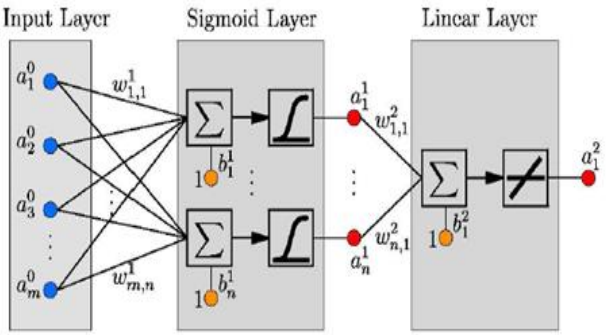

Fig. 2 Feedforward neural network architecture (Most and Bucher 2007)

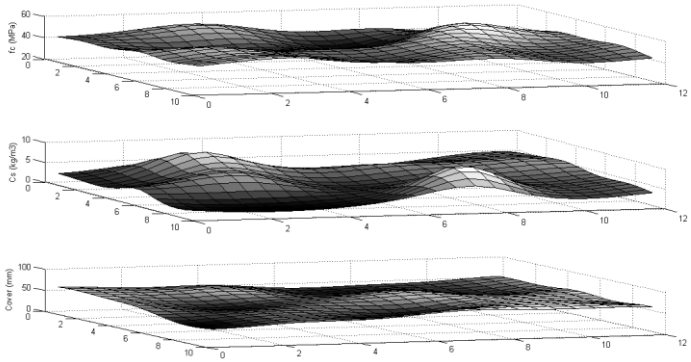

Fig. 3 Random realization of spatial variation ofcover depth of concrete deck

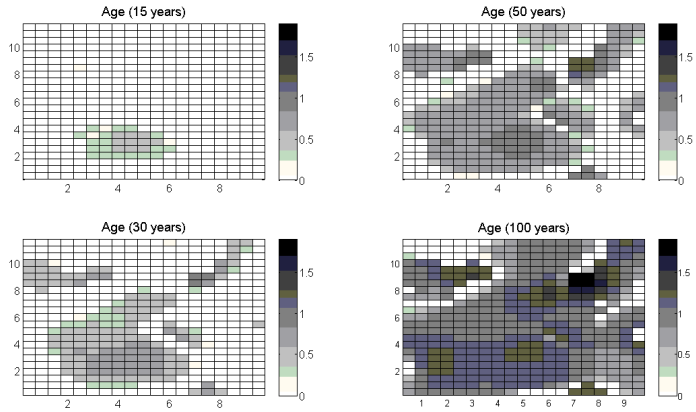

Fig. 4 Random realization of spatial variation of crack width increase with time

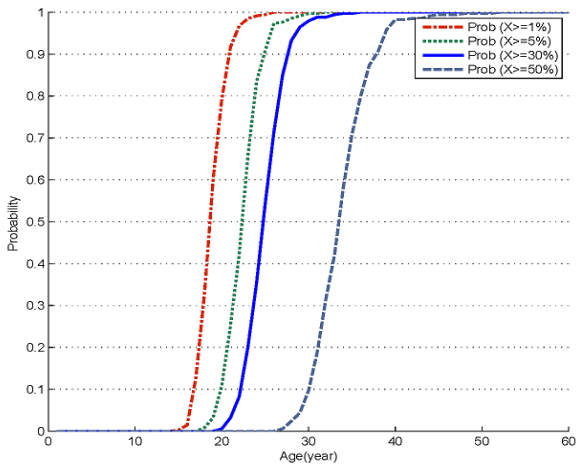

Fig. 5 Probability of the exceeding extent of cracked area from an acceptable threshold

elements for which the condition $[t > Tint(j) + \mathrm{Tsc}(j)]$ is true. Hence $X(t)$, i.e., extent of damage, is a dependent random variable

The developed code in MATLAB carries out Monte Carlo simulation in the space of independent standard normal variables of discretized random fields. Fig. 3 represents a random realization of spatial variability of concrete cover depth, concrete compressive strength and surface chloride concentration as independent random fields.

The result of this Monte Carlo analysis is depicted in Fig. 4 where a random realization of the crack width increase in the elements of the bridge deck system is represented. It is obvious that in every cycle of Monte Carlo simulation another realization may occur. The proportion of the failed area to the whole deck area in every cycle of the Monte Carlo simulation results in a random variable $X(t)$, which representsthe extent of damage.

The most important result of time-dependent spatial reliability analysis is that the probability of exceeding the extent of failure from an acceptable threshold can be calculated. In Fig. 5 the results of such an analysis are represented for various acceptable limits of $X(t)$. In risk-based maintenance management of bridges this can be a rational criterion in selecting optimum life cycle repair and maintenance strategies. For example, if $X(t) = 30\%$ is the acceptable extent of failed area, while there will be negligible risk prior to the age of 20 years, it will increase dramatically and at the age of 30 years this probability will be about 95 percent.

6.3 Neural networks

The structure, input and outputs of developed neural networks are explained in Section 3. A total number of 1000 data sets are produced using Latin hypercube sampling method from which 70% is used in random for training of ANNs and two batches of 15% for validation and testing of the performance of the networks respectively.

Training set is used to adjust the weights on the neural network. Validation set is used to minimize overfitting. It is verified that if any increase in accuracy over the training data set actually yields an increase in accuracy over validation data set that has not been shown to the network before. If the accuracy over the training data set increases, but the accuracy over the validation data set stays the same or decreases, then overfitting occurs and training should be stopped. Testing set is used only for testing the final solution in order to confirm the actual predictive power of the network.

In Fig. 6, the results of regression between predicted and target values of the first ANN are illustrated for example. As it is shown the R factors of the regression are more than 0.99 for three datasets of training, validation and testing which means very good training and generalization of trained ANN. After successful training ANN can be used as a surrogate to the Monte Carlo simulation. This is the same for the other ANN, calculating the crack width during service life.

After training and testing of ANNs, for every discretized element of deck, these networks are used for simulation of the crack initiation time and crack width in every time step during the life cycle. The precision of the trained ANNs is very promising. Fig. 7 represents the close conformance of simulated crack width of the crude Monte Carlo method and trained ANN for one randomly selected discretized element.

The precision of the method is reported once again in Fig. 8, comparing two methods, the pattern of cracked area of the deck in one of the realizations, i.e., one random data point of the simulation, is in very close conformance to that of Monte Carlo simulation during whole service life. These results show very good performance of ANNs, in terms of precision, as surrogates to

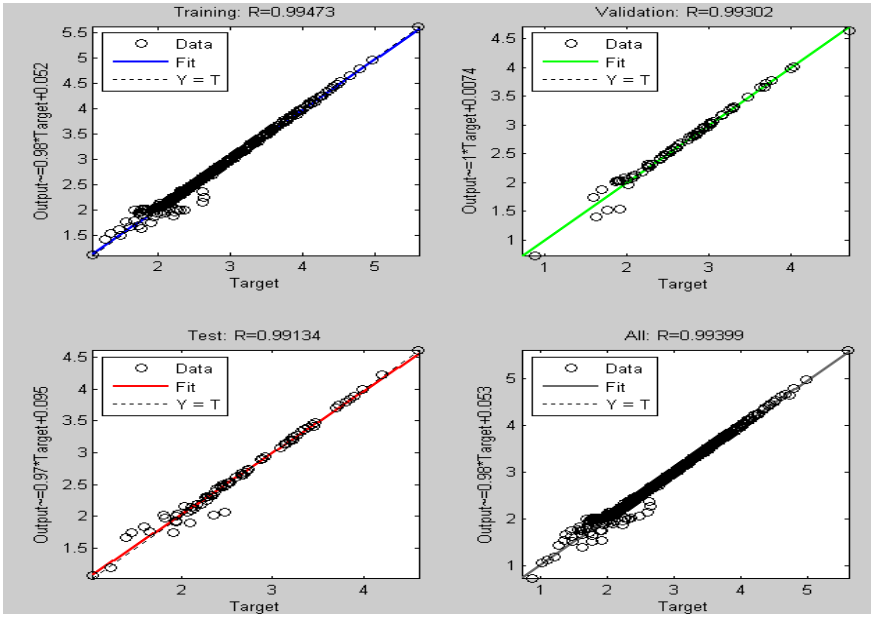

Fig. 6 Regression of ANN output and Latin hypercube simulation results as target values

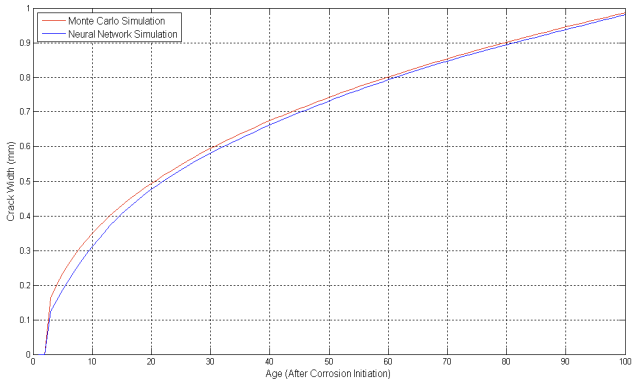

Fig. 7 Conformance of Monte Carlo simulated crack width with that of ANN

the Monte Carlo simulation.

But as the main motivation of this study, saving time in computation is of interest. In this sample analysis using well trained ANNs means decreasing the time of computation in the order of 7 to 8 times. Using an Intel ® Core 2 Due, 2.2 GHz CPU, the full analysis with the proposed method takes about 70 minutes while it is completed in about 550 minutes via crude Monte Carlo simulation with 10^6 iterations. This is because of the time-consuming iterative solution of nonlinear simultaneous equations needed for crack width calculation according to the analytical model. It shall be noted that application of this method for bridges with large deck areas, and or considering strength limit states, which require more sophisticated structural analyses, the proposed method will be more attractive.

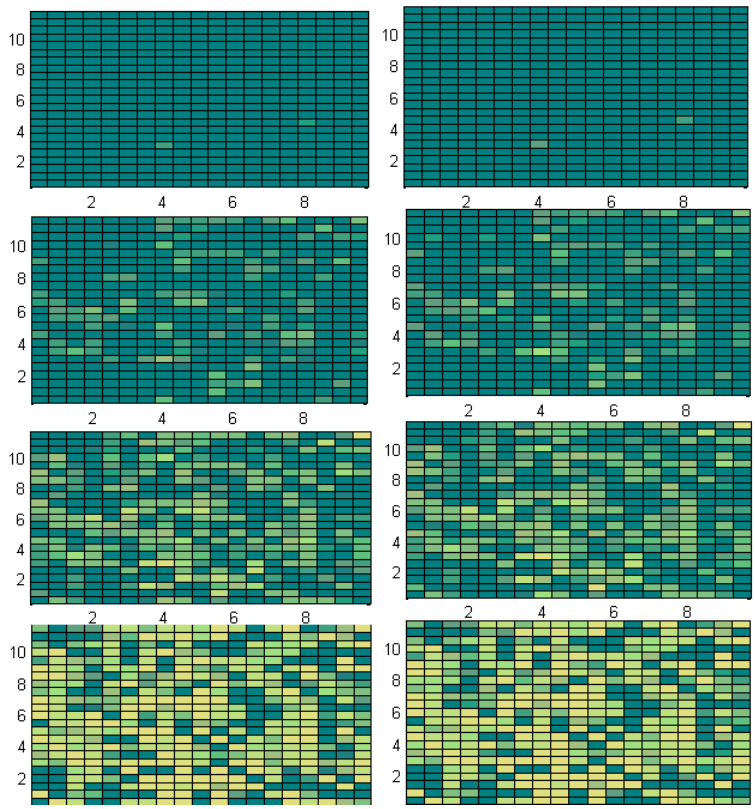

Fig. 8 Random realization of spatial variation of crack width at age 15, 30, 50 and 100 years of service life, (a) results of Monte Carlo simulation, (b) results of Neural Network simulation

7. Conclusions

In this paper, first the spatial time-dependent reliability analysis of the RC bridge decks subject to chloride ingress is studied. The spatial variability of concrete cover depth, compressive strength and surface chloride concentration was considered whilst other material and deterioration parameters were treated as dependent random fields or random variables. The results of the analysis are presented as the extent and likelihood of the corrosion damage during the life cycle of a hypothetical bridge deck. Since the Monte Carlo simulation is a time consuming and inefficient method working on random fields, the utility of neural networks as a surrogate is investigated. In summary, the following conclusion can be made

Ⅰ. The proposed spatial-temporal variable analysis yields to the prediction of extent and likelihood of damage. This is an invaluable data in decision making about maintenance management of bridges.

Ⅱ. The analytical model used for crack width calculation requires iteratively solving simultaneous equations in every time step. In the Monte Carlo simulation method, these equations shall be solved many times for every discretized element. Consequently, spatial time-dependent reliability analysis is very time consuming. The precision of simulated crack initiation time and crack width using trained ANNs is very rewarding and the results are in well conformance with

those of Monte Carlo simulation.

Ⅲ. The merit of the proposed method is in its efficiency in terms of the required time for simulation. Based on the prescribed precision, the efficiency increases in the order of 8times compared to the crude Monte Carlo method. This method may be even more interesting dealing with strength limit states, e.g. flexural failure of a bridge deck, which require more sophisticated reliability analysis.

References

American Concrete Institute, ACI 365 1R-00 (2000), Service Life Prediction, State of the Art Report, Detroit, USA.

American Concrete Institute, ACI (2005), Building Code Requirements for Structural Concrete, ACI 318-05, Detroit, USA.

Bamforth, P.B. and Price, W.F. (1996), "An international review of chloride ingress into structural concrete", *Taywood Engineering Ltd.,Technology Division*, Middlesex.

Bentz, E.C. (2003), "Probabilistic modeling of service life for structures subjected to chlorides", *ACI Mater. J.*, **100**(5), 391-397.

Chen, D. and Mahadevan, S. (2008), "Chloride-induced reinforcement corrosion and concrete cracking simulation", *Cement Concrete Compos.*, **30**, 227-238.

Cheng, J, Li, Q.S. and Xiao, R.C. (2008), "A new artificial neural network-based response surface method for structural reliability analysis", *J. Struct. Eng. Mech.*, **23**, 51-63.

Chryssanthopoulos, M. and Sterritt, G. (2002), "Integration of deterioration modeling and reliability assessment for reinforced concrete bridge structures", First ASRANet international colloquium (CD-ROM).

Duprat, F. (2007), "Reliability of RC beams under chloride ingress", *Constr. Build. Mater.*, **21**, 1605-1616.

Duracrete (2000), Final Technical Report: Probabilistic performance based durability design of concrete structures, The European Union- BriteEuRam III.

El Maaddawy, T. and Soudki, K. (2007), "A model for prediction of time from corrosion initiation to corrosion cracking", *Cement Concrete Compos.*, **29**(3), 168-175.

Engelund, S. and Sorensen, J.D. (1998), "A Probabilistic model for chloride ingress and initiation of corrosion in reinforced Concrete Structures", *Struct. Safety*, 2**0**, 69-89.

Fib (CEB-FIP)(2006), Model Code foe Service Life Design.

Frangopol, D.M., Lin, K.Y. and Estes, A.C. (1997), "Life-cycle cost design of deteriorating structures", *J. Struct. Eng. ASCE*, **123**, 1390-1401.

Hagan, M.T., Demuth, H. and Beale, M. (1996), Neural Network Design, PWS Publishing Company.

Hornik, K. (1991), "Approximation capabilities of multilayer feedforward networks", *Neural Networks*, **4**(2), 251-257

Hurtado, J.E. and Alvarez, D.A. (2001), "Neural network based reliability analysis: A comparative study", *Comput. Meth. Appl. Mech. Eng.*, **191**, 113-132

Hurtado, J.E. (2002), "Analysis of one-dimensional stochastic finite elements using neural networks", *Probabil. Eng. Mech.*, **17**, 35-44.

Karimi, A.R., Ramachandran, K. and Buenfeld, N. (2005), "Probabilistic analysis of reinforcement corrosion with spatial variability using random field theory", *Proceedings of the Ninth International Conference on Structural Safety and Reliability*, ICOSSAR 05. Rome, Italy.

Kong, J.K. Ababneh, A.N., Frangopol, D.M. and Xi, Y. (2002), "Reliability analysis of chloride penetration in saturated concrete", *Probabil. Eng. Mech.*, **17**, 305-315.

Li, C. and Der Kiureghian, A. (1993), "Optimal discretization of random fields", *J. Eng. Mech. ASCE*, **119**, 1136-1154.

Li, C.Q. (2003), "Life cycle modeling of corrosion affected concrete structures-propagation", *J. Struct. Eng., ASCE*, **129**(6) ,753-776.
Li, C.Q., Melchers, R.E. and Zheng J.J. (2006), "Analytical model for corrosion-induced crack width in reinforced concrete structures", *ACI Struct. J.*, **103**(4), 479-487.
Li, Y., Vrouwenvelder, T., Wijnants, G.H. and Walraven, J. (2004), "Spatial variability of concrete deterioration and repair strategies", *Struct.Concrete*, **5**(3), 121-130.
Liu, Y. and Weyers, R.E. (1998), "Modeling the time-to-corrosion cracking in chloride contaminated reinforced concrete structures", *ACI Mater J.*, **95**(6), 675-181.
McKay, M.D., Conover, W.J. and Beckman, R.J. (1979), "A comparison of three methods for selecting values of input variables in the analysis of the output from a computer code", *Technometrics*, **21**(2), 239-245.
Most, T. and Bucher, C. (2007), "Probabilistic analysis of concrete cracking using neural networks and random fields", *Probabil. Eng. Mech.*, **22**, 219-229.
Nataf, A. (1962), "Détermination des distributions de probabilities don't les margessontdonnées", ComptesRendus de l'Academie des Sciences, **225**, 42-43.
Olsson, A., Sandberg, G. and Dahlblom, O. (2003), "On Latin hypercube sampling for structural reliability analysis", *Struct. Safety*, **25**, 47-68.
Papadakis, V.G., Roumeliotis, A.P., Fardis, M.N. and Vagenas, C.G. (1996), "Mathematical modeling of chloride effect on concrete durability and protection measures", (Eds. Dhir, R.K. and Jones, M.R.) Concrete repair, rehabilitation and protection, London.
Papadrakakis, M., Papadopoulos, V. and Lagaros, N.D. (1996), "Structural reliability analysis of elastic-plastic structures using neural networks and monte carlo simulation", *Comput. Meth. Appl. Mech. Eng.*, **136**, 145-163.
Poupard, O., L'Hostis, V., Catinaud, S. and Petre-Lazar, I. (2006), "Corrosion damage diagnosis of a reinforced concrete beam after 40 years natural exposure in marine environment", *Cement Concrete Res.*, **36**, 504-520.
Schueller, G.I. (1997), "A state of-the-art report on computational stochastic mechanics", *Probabil. Eng. Mech.*, **12**(4),197-231.
Stewrat, M.G. and Mullard, J.A. (2008), "Spatial time-dependent reliability analysis of corrosion damage and the timing of first repair for RC structures", *Eng. Struct*, **29**(7), 1457-1464
Sudret, B., Defaux, G. and Pendola, M. (2007), "Stochastic evaluation of the damage length in RC beams submitted to corrosion of reinforcing steel", *Civil Eng. Envir. Syst.*, **24**(2),165-178.
Sudret, B. and Der Kiureghian, A. (2000), "Stochastic finite element methods and reliability: a state of the art report", *Department of Civil and Environmental Engineering University of California*, Berkeley.
VanMarcke, E. (1984), *Random fields*, analysis and synthesis, MIT Press.
Vu, K.A.T., Stewart, M.G. and Mullard, J. (2005), "Corrosion-induced cracking: experimental data and predictive models", *ACI Struct. J.*, **102**(5), 719-726.
Vu, K.A.T. and Stewart, M.G. (2005), "Predicting the likelihood and extent of reinforced concrete corrosion-induced cracking", *J. Struct. Eng.*, **131**(11), 1681-1689.

CC